

Structural robustness of networks with degree-degree correlations between second-nearest neighbors

Yuka Fujiki^{1,2,*} and Stefan Junk^{3,†}

¹*Frontier Research Institute for Interdisciplinary Sciences (FRIS),
Tohoku University, 6-3 Aramaki aza Aoba, Aoba-ku, Sendai 980-8578, Japan*

²*Advanced Institute for Materials Research (AIMR),
Tohoku University, 2-1-1 Katahira, Aoba-ku, Sendai, 980-8577 Japan*

³*Gakushuin University, 1-5-1 Mejiro, Toshima-ku, Tokyo 171-8588 Japan*

(Dated: December 4, 2024)

We numerically investigate the robustness of networks with degree-degree correlations between nodes separated by distance $l = 2$ in terms of shortest path length. The degree-degree correlation between the l -th nearest neighbors can be quantified by Pearson's correlation coefficient r_l for the degrees of two nodes at distance l . We introduce l -th nearest-neighbor correlated random networks (l -NNCRNs) that are degree-degree correlated at less than or equal to the l -th nearest neighbor scale and maximally random at farther scales. We generate 2-NNCRNs with various r_1 and r_2 using two steps of random edge rewiring based on the Metropolis-Hastings algorithm and compare their robustness against failures of nodes and edges. As typical cases of homogeneous and heterogeneous degree distributions, we adopted Poisson and power law distributions. Our results show that the range of r_2 differs depending on the degree distribution and the value of r_1 . Moreover, comparing 2-NNCRNs sharing the same degree distribution and r_1 , we demonstrate that a higher r_2 makes a network more robust against random node/edge failures as well as degree-based targeted attacks, regardless of whether r_1 is positive or negative.

I. INTRODUCTION

Many complex networks in the real world share a common property that the distribution of the number of edges (degree) from each node is approximated by a power-law function, which is known as the scale-free property [1]. The degree correlation among nodes in such networks, particularly nearest-neighbor degree correlation (NNDC), influences network behavior, including robustness to node and edge failures, the spread of infections, and oscillator synchronization [2–4].

Additionally, recent studies have shown that the majority of complex networks in the real world exhibit long-range degree correlations (LRDCs) at greater distances than next-nearest neighbors [5]. While some LRDCs can be explained as “extrinsic” LRDCs resulting from the propagation of the NNDCs, for the most part, these are “intrinsic” LRDCs that are not merely consequences of the NNDCs [6]. The effects of LRDCs remain poorly understood, except for some special cases. For example, it is known that the shortest path length between high-degree nodes influences network functions and dynamical properties [7–12], and that transsportative structures (degree correlations between two neighbors of a node) can amplify the majority illusion [13]. Towards understanding the relationship between network properties and LRDCs, in this study, we numerically investigate the influence of LRDC at shortest path distance $l = 2$ on the structural robustness, which is one of the most fundamental properties of networks.

Robustness refers to the ability of a network to maintain its overall structural and functional integrity against node or edge removal [14–18]. This concept may be interpreted as assessing the stability of network functioning, or the difficulty of eradicating infectious diseases and misinformation spreading on the network. Taking only the degree distribution of a network into account, analytical calculations using the mean-field approximation show that networks with homogeneous degree distributions lose global connectivity earlier, i.e., after a smaller percentage of random failures, than heterogeneous degree distributions [19, 20]. On the other hand, it is known that heterogeneous networks are more vulnerable to targeted attacks than homogeneous ones [21, 22]. Beyond the effect of the degree distribution, it is known that positive, resp. negative, NNDCs makes the network more robust, resp. weaker, [23–26]. If LRDCs influence robustness in a manner similar to NNDCs, this understanding would provide valuable insights into the resilience of networks and contribute to more effective system design.

* yfujiki@tohoku.ac.jp

† sjunk@math.gakushuin.ac.jp

For this purpose, we introduce l -th nearest-neighbor correlated random networks (l -NNCRNs) that are degree-degree correlated up to the l -th nearest-neighbor distance and maximally random at any further scale. In particular, the difference between l -NNCRNs and $(l - 1)$ -NNCRNs is caused by intrinsic LRDCs at distance l .

Formally, LRDCs at distance l can be characterized by the conditional probability $P(k, k'|l)$ that the degrees of two nodes are k and k' given that the two nodes are at distance l from each other in terms of the shortest path length, see Sec. II A below. Thus, to isolate the effect of LRDCs at a distance l , we can compare properties of l -NNCRNs to networks with the same correlations $P(k, k'|l')$ at distances $l' \leq l - 1$ and no intrinsic correlations at distance l . The strength of degree correlations at distance l is quantified by Pearson's correlation coefficient r_l for $P(k, k'|l)$.

We numerically implement this framework in the case $l = 2$ for a representative choice of correlations. Our results demonstrate, firstly, that the correlations at distances $l = 0$ and $l = 1$, i.e. the degree distribution and r_1 , place some constraints on the range of r_2 . We then perform random node or edge removal and degree-based targeted attack on networks and quantify the robustness based on the percolation critical point p_c and the robustness measure R introduced by Schneider *et al.* [27].

Qualitatively, our results suggest that the critical point p_c shifts with r_2 when the correlations at shorter distances are kept fixed, which proves that LRDCs indeed influence network robustness. The effect of r_2 on robustness follows a similar trend to that of r_1 . Networks with larger r_2 tend to be more robust against both random node/edge failure and degree-based targeted attacks when the robustness is quantified by $f_c = 1 - p_c$. Using another measure of robustness, R , networks with larger r_2 are more fragile against random node/edge failure but remain more robust against degree-based targeted attacks. The difference is because both measures quantify slightly different aspects of robustness, as will be explained in Sec III B. Quantitatively, the influence of r_2 on network robustness is weaker than that of r_1 , but it is generally on a comparable order. To clarify how degree correlations at distance $l = 2$ affect network robustness, we decompose 2-NNCRNs into k -cores and confirm that a strongly positive r_2 induces a core, which is as robust as the core induced by r_1 . We close the discussion by investigating the values of r_2 exhibited by real networks and the possibility for optimization of robustness based on LRDCs.

The manuscript is organized as follows. In Sec. II we define l -NNCRNs by quantifying LRDCs using $P(k, k'|l)$ and r_l . Moreover, we explain the algorithm for generating 2-NNCRNs with various values of r_l using random edge rewiring based on the Metropolis-Hasting algorithm. Sec. III presents the numerical results obtained from our simulations, including the effects of LRDCs on network robustness and the relationship between r_1 , r_2 and the degree distribution. Finally, in Sec. IV we summarize our key findings and propose avenues for future research in elucidating the role of LRDCs in complex networks.

II. NUMERICAL METHOD

We numerically sample networks with various degree-degree correlations between nodes at distance $l \leq 2$ in terms of shortest path length.

We propose l -th nearest neighbor correlated networks (l -NNCRNs), which are random at shortest path distances greater than l and which serve as an idealized model to study the relation between network robustness and LRDCs without other confounding factors. 2-NNCRNs are sampled using a three-step edge-rewiring algorithm to fix, successively, the degree sequence, the NNDCs and finally the LRDCs at distance $l = 2$. The definition and sampling method of l -NNCRNs are explained in the following two subsections.

Note that in real-world networks, the effect of r_2 is complicated by the fact that r_1 by itself also influences network robustness and, on the other hand, constrains the range of r_2 . In addition, intrinsic long-range correlations at distances $l \geq 3$ may exist and affect robustness. 2-NNCRNs do not have such intrinsic long-range correlations at distances $l \geq 3$, allowing us to isolate the effects of r_1 and r_2 . Moreover, by preparing 2-NNCRNs with identical r_1 but varying r_2 , we can focus specifically on the effect of r_2 . This idealized model enables us to disentangle these effect and to demonstrate that LRDCs at distance $l = 2$ can have a profound effect on network robustness. To investigate the relation between the robustness and LRDCs at $l = 2$, we compare the effect of random node/edge removal and of degree-based targeted attack on the network structure in 2-NNCRNs with different degree correlations. The analysis of these properties is explained in the final subsection.

A. Definition of l -NNCRNs

To analyze LRDCs in a given network, we first need to understand maximally random networks that have the same nearest-neighbor correlations as the network [6]. We can use that model as a baseline to judge whether the degree

correlations at greater distances than $l = 1$ are just extrinsically caused by the NNDCs or whether they are intrinsic. Extending this, we call a network ensemble l -NNCRN if it is degree-degree correlated at less than or equal to the l -th nearest neighbor distance and maximally random at any further scale. A nearest-neighbor correlated random network is thus a 1-NNCRN.

The conditional probability $P(k, k'|l)$ that two randomly chosen nodes separated at a distance l have degree k and k' describes the LRDCs at distance l . Since the conditional probability is a high-dimensional matrix and not easy to interpret, we use the Pearson's correlation coefficient r_l for the degrees of two nodes at distance l as a convenient observable that quantifies the strength of the l -th nearest neighbor degree correlation. It is defined as

$$r_l = \frac{\sum_{k,k'} kk' P(k, k'|l) - [\sum_{k,k'} k P(k, k'|l)]^2}{\sum_{k,k'} k^2 P(k, k'|l) - [\sum_{k,k'} k P(k, k'|l)]^2} \in [-1, 1], \quad (1)$$

where the sum is over all possible degrees. It can also be represented as

$$r_l = \frac{\frac{1}{2M^{(l)}} \sum_{i,j} \delta_{\text{dist}(i,j),l} k_i k_j - \left[\frac{1}{2M^{(l)}} \sum_{i,j} \delta_{\text{dist}(i,j),l} k_i \right]^2}{\frac{1}{2M^{(l)}} \sum_{i,j} \delta_{\text{dist}(i,j),l} k_i^2 - \left[\frac{1}{2M^{(l)}} \sum_{i,j} \delta_{\text{dist}(i,j),l} k_i \right]^2}. \quad (2)$$

Here, the sum is over all nodes, $\text{dist}(i, j)$ is the shortest path distance between i and j . The term $M^{(l)}$ is defined as

$$M^{(l)} = \frac{1}{2} \sum_{i,j} \delta_{\text{dist}(i,j),l}, \quad (3)$$

where $\delta_{d,l}$ is Kronecker δ . In the case of $l = 1$, this quantity is known as assortativity [2] and it has been extended to arbitrary $l > 1$ by [28, 29].

Note that the NNDCs can induce extrinsic LRDCs at distance $l = 2$, so that the value of r_2 may differ from zero even if the network is a 1-NNCRN. For a given network, we thus define r_2^{ext} to be the average value of r_2 among networks with the same degree sequence and NNDC, as described by $P(k, k'|l = 1)$. We say that a network is intrinsically degree-degree correlated at $l = 2$ if the value of r_2 significantly differs from r_2^{ext} .

B. Edge rewiring algorithm

Edge rewiring algorithms are widely used to investigate graph structures [30–32]. Through randomization via rewiring, the algorithm can generate the most randomized network ensembles under specific constraints. In this study, given parameters J_1 and J_2 , we generate 2-NNCRNs through the following sequence of steps based on the Metropolis-Hasting algorithm started with an initial network G_0 : (1) Rewire edges while preserving the degree sequence to generate a 1-NNCRN G_1 (see Algorithm 1). (2) Rewire edges in the resulting network while preserving the NNDC (i.e., $P(k, k'|l = 1)$) to generate a 2-NNCRN G_2 (see Algorithm 2).

Note that when choosing edges, we (temporarily) equip each edge with an orientation. We also mention that the rewiring in Algorithm 1 is irreducible for the set of graphs with the same degree sequence and that in Algorithm 2 is as well for the NNDC [33, 34]. Moreover, the reason why we include Step 2 in both algorithms is to ensure that the Markov chains are aperiodic and thus converge to equilibrium.

These algorithms generate a canonical ensemble of networks in the sense of statistical physics, which satisfies a constraint in terms of the mean value (soft constraint) and belongs to the general class of exponential random graph models [35–37].

Algorithm 1 Generating a 1-NNCRN while preserving the degree sequence

- 1: Increase time step by 1.
 - 2: Return to step 1 with probability $1/2$.
 - 3: Randomly choose two edges (u_1, u_2) and (v_1, v_2) .
 - 4: If rewiring $(u_1, u_2) \rightarrow (u_1, v_2)$ and $(v_1, v_2) \rightarrow (v_1, u_2)$ creates a loop or a multi-edge, return to step 1.
 - 5: Compute the current value r_1^{rev} of r_1 , the value r_1^{ext} of r_1 after rewiring $(u_1, u_2) \rightarrow (u_1, v_2)$ and $(v_1, v_2) \rightarrow (v_1, u_2)$, and the transition probability $P(u_1, u_2, v_1, v_2) = \min(1, \exp[-J_1(r_1^{\text{ext}} - r_1^{\text{rev}})])$.
 - 6: With probability $P(u_1, u_2, v_1, v_2)$, rewire edges $(u_1, u_2) \rightarrow (u_1, v_2)$ and $(v_1, v_2) \rightarrow (v_1, u_2)$.
 - 7: Repeat steps 1–6 until the system reaches equilibrium.
-

Algorithm2 Generating a 2-NNCRN while preserving the degree sequence and $P(k, k'|l = 1)$

- 1: Increase time step by 1.
 - 2: Return to step 1 with probability 1/2.
 - 3: Randomly choose an edge (u_1, u_2) .
 - 4: Randomly choose another edge (v_1, v_2) such that v_1 has the same degree as u_1 .
 - 5: If rewiring $(u_1, u_2) \rightarrow (u_1, v_2)$ and $(v_1, v_2) \rightarrow (v_1, u_2)$ creates a loop or a multi-edge, return to step 1.
 - 6: Compute the current value r_2^{rev} of r_2 , the value r_2^{ext} of r_2 after rewiring $(u_1, u_2) \rightarrow (u_1, v_2)$ and $(v_1, v_2) \rightarrow (v_1, u_2)$, and the transition probability $P(u_1, u_2, v_1, v_2) = \min(1, \exp[-J_2(r_2^{ext} - r_2^{rev})])$.
 - 7: With probability $P(u_1, u_2, v_1, v_2)$, rewire edges $(u_1, u_2) \rightarrow (u_1, v_2)$ and $(v_1, v_2) \rightarrow (v_1, u_2)$.
 - 8: Repeat 1–7 until the system reaches equilibrium.
-

More precisely, in Algorithm 1 the degree of each node does not change, so the degree sequence acts as a hard constraint. On the other hand, the rewiring generates a set of networks with different NNDCs but which is random at further distances, i.e., a 1-NNCRNs. The mean value of r_1 is a soft constraint in Algorithm 1 and in equilibrium a configuration G_1 (with the same degree sequence as the initial network G_0) appears with probability

$$\Pi_1(G_1|G_0) = \frac{e^{-J_1 r_1(G_1)}}{Z_1(J_1|G_0)}, \quad (4)$$

where $r_1(G)$ is the value of r_1 for G and Z_1 is the partition function

$$Z_1(J_1|G_0) = \sum_{G'} e^{-J_1 r_1(G')}. \quad (5)$$

The mean value of r_1 is zero in the case $J_1 = 0$ and moves in the positive/negative direction with J_1 . Moreover, when the network size is sufficiently large, the value of r_1 tends to be narrowly distributed around its mean value (notice that the error bars in Fig 1 are barely visible).

The idea behind Algorithm 2 is similar, but in addition to the degree sequence the condition that u_1 and v_1 have the same degree ensures that $P(k, k'|l = 1)$ is preserved, and in particular that r_1 remains constant. When the system reaches equilibrium in Algorithm 2, a configuration G_2 with the same degree sequence and NNDC as G_1 appears with probability

$$\Pi_2(G_2|G_1) = \frac{e^{-J_2 r_2(G_2)}}{Z_2(J_2|G_1)}, \quad (6)$$

where $r_2(G)$ is the value of r_2 for G and $Z_2(J_2|G_1)$ is the partition function in the form of

$$Z_2(J_2|G_1) = \sum_{G'} e^{-J_2 r_2(G')}. \quad (7)$$

The mean value of r_2 equals r_2^{ext} in the case $J_2 = 0$ and moves in the positive/negative direction in accordance with J_2 . Both rewiring procedures satisfy the detailed balance condition. Thus, after successively applying Algorithms 1 and 2 to an initial network G_0 until equilibrium is reached, we obtain network G_2 with probability

$$\sum_{G_1} \Pi_1(G_1|G_0) \Pi_2(G_2|G_1). \quad (8)$$

We prepare two kinds of random networks as the initial network G_0 , which prescribes the degree distribution of the network and which is preserved by Algorithms 1 and 2. The first is the Erdős-Rényi random graph model, whose degree distribution is approximated by a Poisson distribution $P(k) = \langle k \rangle^k e^{-k}/k!$ when the network is large enough. We set the number of nodes and the average degree at $N = 20,000$ and $\langle k \rangle = 5.0$, respectively. The second is the configuration model [38] with a power-law degree distribution $P(k) = ck^{-\gamma}$ with the number of nodes $N = 20,000$, the power-law exponent $\gamma = 2.5$, the minimum degree $k_{min} = 2$, and the structural cutoff $k_c = \sqrt{N}$ [39], where c is the normalization constant.

While the former network belongs to the group of networks with homogeneous degree distribution, the later is a network with power-law degree distribution, which is one of the common features shared by many real-world complex networks. Empirically, power law exponents in the range $2 \lesssim \gamma \lesssim 4$ are common. Such a heterogeneous degree distribution tends to amplify the effect of degree-degree correlations on robustness and other properties of networks. Hereafter, we refer to these networks as Poisson and power-law networks, respectively.

C. Analyzing the structural robustness

The structural robustness of networks assesses the ease with which the global connectivity of the network is maintained. There are several strategies for destroying networks and processes of how networks fail [20–22, 40]. Here, we investigate the most straightforward mechanisms, namely random node/edge failures, as well as targeted attacks removing nodes in decreasing order of degree.

As the fraction p of remaining nodes/edges decreases, the size of the largest connected component $N_{LCC}(p)$ in the network decreases as well. For the network to maintain its functionality, global connectivity is necessary. Thus the value of p at which the largest connected component collapses, the critical point p_c , serves as an essential indicator of robustness. We find it more intuitive to evaluate robustness using the fraction of removed nodes/edges required for collapse, $f_c = 1 - p_c$, so that a larger value of f_c indicates that the network is more robust.

In this study, the network size is fixed at $N = 20,000$ and we approximate the critical point p_c using a threshold of $p_{0.005} = \sup\{p: \langle N_{LCC}(p) \rangle < 0.005N\}$ where the giant component size reaches 0.5% of the total to approximate the critical point p_c . Moreover, we use $f_{0.005} = 1 - p_{0.005}$ as a robustness measure.

In practice, $N_{LCC}(p)$ does not always rapidly decrease around a single value of p . More precisely, the network may contain a densely connected core whose percolation occurs later than the more loosely connected periphery, which results in multiple phase transitions. The threshold $p_{0.005}$ has been chosen to detect the “true” collapse of network connectivity where all connected components become sublinear in the network size N . To illustrate this phenomenon, we compute the susceptibility

$$\chi(p) = \frac{\langle N_{LCC}^2(p) \rangle - \langle N_{LCC}(p) \rangle^2}{\langle N_{LCC}(p) \rangle}. \quad (9)$$

The peak of the susceptibility suggests the location of critical points in a continuous phase transition and is often used to approximate p_c . However, in situations as described above the susceptibility exhibits multiple peaks how relative sizes can flip as the network size increases, which makes it unsuitable for quantifying robustness. The multiple peaks phenomenon can be seen in the bottom right panel in Fig. 3.

Beyond the critical point, the size of the giant component as p varies also carries important information. Schneider *et al.* [27] proposed the area $R = \int_0^1 S(p)dp$ under the curve $S(p) = N_{LCC}(p)/N$ as a robustness measure. A larger value of $S(p)$ indicates that the network is more robust for any fixed fraction p of remaining nodes/edges and R thus measures the average robustness away from p_c .

In summary, network robustness can be interpreted using two measures: $f_{0.005}$ and R . A larger value of $f_{0.005}$ indicates that the network can maintain its global connectivity under a higher fraction of node/edge removals. The robustness measure R , defined as the area under the curve $S(p)$, reflects the average connectivity across all node/edge removal scenarios, with a larger R indicating greater robustness.

To evaluate $f_{0.005}$ and R in a given network, we use the method proposed by Newman and Ziff [41].

III. RESULT

In this section, we present the results of the numerical calculations based on the method described in Sec. II B. First, we confirm that the algorithm works as desired, i.e., that the generated 2-NNCRNs exhibit various degree-degree correlations between both nearest-neighbor nodes and second-nearest-neighbor nodes. Next, we assess their robustness against random node/edge failures and degree-based targeted attacks.

A. Constraints on degree correlations in 2-NNCRNs

The purpose of this section is to give some details about the networks obtained by the rewiring procedure explained above, and in particular to explain how the parameters influence the range of correlations achievable with our method. More precisely, we confirm that degree distribution and r_1 impose constraints to r_2 and that the rewiring algorithm can sample network configurations with various r_2 and the same r_1 .

Figure 1 depicts the average values of r_1 and r_2 of 2-NNCRNs generated by the rewiring method described in the previous section starting with an initial network characterized by (a) the Poisson degree distribution and (b) the Power-law degree distribution. As shown in Fig 1, the range of r_2 strongly depends on the degree distribution and r_1 . Let us comment on a few trends:

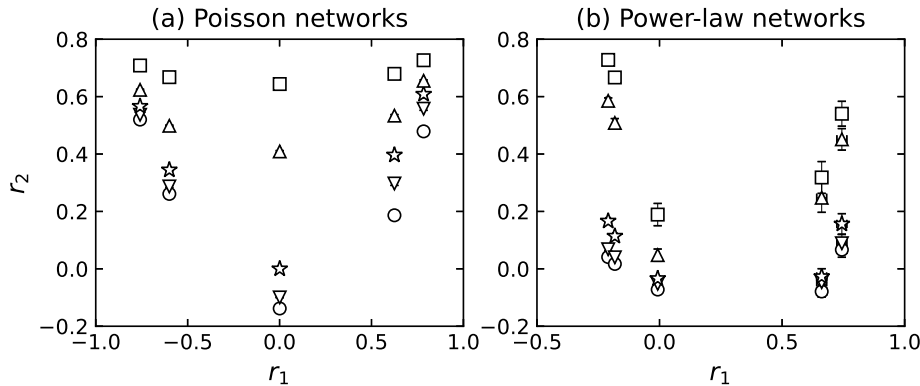


FIG. 1: The mean value of r_1 and r_2 of 2-NNCRNs. Each data point is the average value over 100 configurations, and the error bar is the standard deviation. The r_1 and r_2 of power-law networks exhibit larger error bars than those of Poisson networks, which can be attributed to significant differences in maximum degrees across random seeds. The symbols vary based on the rewiring parameter J_2 . For $J_2 = -2M, -M, 0, M, 2M$, the symbols are a sphere, a downward triangle, a star, an upward triangle, and a box, respectively, where M is the number of edges in each network. In particular, the star indicates $J_2 = 0$, where the value of r_2^{ext} reflects the extrinsic LRDC at $l = 2$ induced by r_1 in 1-NNCRNs. If r_2 is greater than/less than r_2^{ext} , it implies that an intrinsic positive/negative LRDC is present at $l = 2$.

First, we note that r_2 is shifted in the positive direction by larger absolute values of r_1 . Such positive extrinsic LRDCs have also been observed in NNCRNs in [6] and [42] and are consistent with the positive correlation of degrees between nodes at even distances. To understand this effect, note that if r_1 is close to +1, similar degrees tend to be adjacent, leading to similar degrees at $l = 2$ and resulting in higher values of r_2 . On the other hand, if r_1 is close to -1, high degrees tend to be adjacent to low degrees and vice versa. Due to this alternating pattern, we again find that nodes at distance $l = 2$ have similar degrees, which results in high values of r_2 .

Next, we observe that the range of r_2 is narrower if the absolute value of r_1 is large in the case of Poisson degree distributed networks (Fig 1(a)). For power-law networks, the converse is true but the effect is much weaker (Fig 1(b)). In other words, the range of r_2 values achievable by 2-NNCRNs strongly depends on the value of r_1 in Poisson networks, while the same trend is not observed for power-law networks. At present, we do not have a satisfying explanation for this behavior and we conclude that the relationship between r_1 and r_2 is complex and constrained by the degree distribution.

Finally, we mention that neither the range of r_1 nor of r_2 are symmetric. This is not surprising – for example, as explained above, both r_1 close to +1 and r_1 close to -1 tend to induce large positive values for r_2 , but the mechanism is different in both cases.

B. Random failure

Having confirmed our samples to be degree-degree correlated at distances $l = 1$ and $l = 2$ in various ways, we now investigate their robustness using the method described in Sec. II C.

Figs 2–3 depict the relative sizes of the largest connected component $S = \langle N_{\text{LCC}} \rangle / N$ and the susceptibility χ (see Eq. (9)) as functions of the probability p that an edge remains.

The solid black lines in Figs 2–3 represent the case of $J_2 = 0$, i.e., the 1-NNCRNs without intrinsic correlations at distance $l \geq 2$, as the baseline for comparison. With the exception of the rightmost panel of Fig 3, the peak position of susceptibility suggests that p_c increases with larger r_2 -values, for fixed r_1 .

As discussed in Sec II C, there may be two peaks in susceptibility in the power-law networks with $r_1 = 0.74$, see the bottom right panel of Fig 3. The first peak appears at $p = 0.052$ and is independent of r_2 , while the second peak appears at larger p and varies with r_2 . Moreover, the direction of change (i.e., the qualitative effect of r_2 on the location of the peak), is opposite to the behavior mentioned before. Double-peak transitions have been reported in networks with high clustering coefficients [43], and they are known to be characteristic of networks with a core-periphery structure. The first peak signifies the emergence of a dense core giant component dominated by high-degree

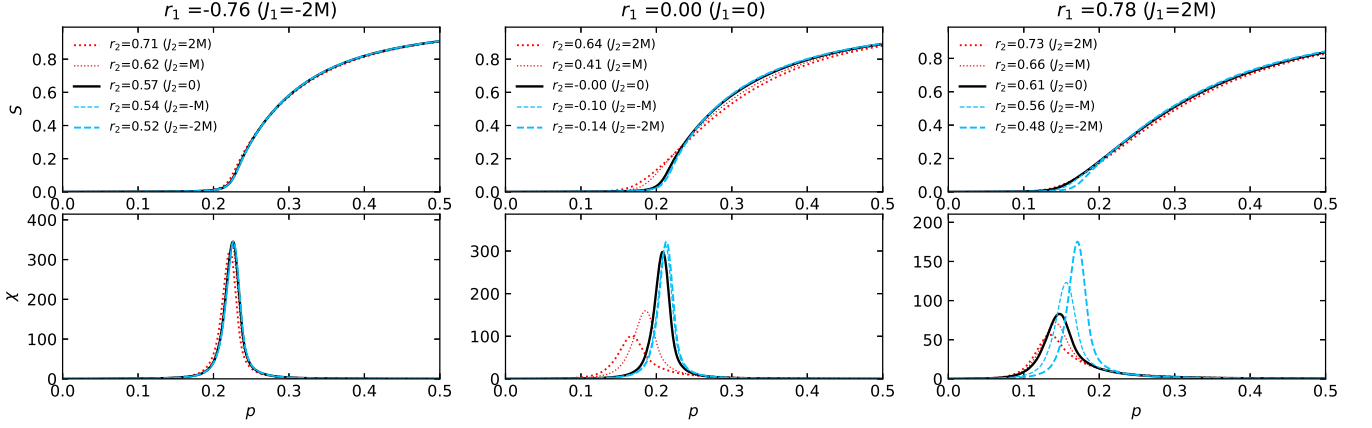


FIG. 2: The S and χ dependence on the edge remaining probability p during random edge failure on 2-NNCRNs with Poisson degree distribution. The set of 2-NNCRNs is the same as in Fig 1(a). The left, middle, and right panels correspond to rewiring parameters $J_1 = -2M, 0,$ and $2M$, respectively. The colors and types of the lines correspond to rewiring parameters J_2 .

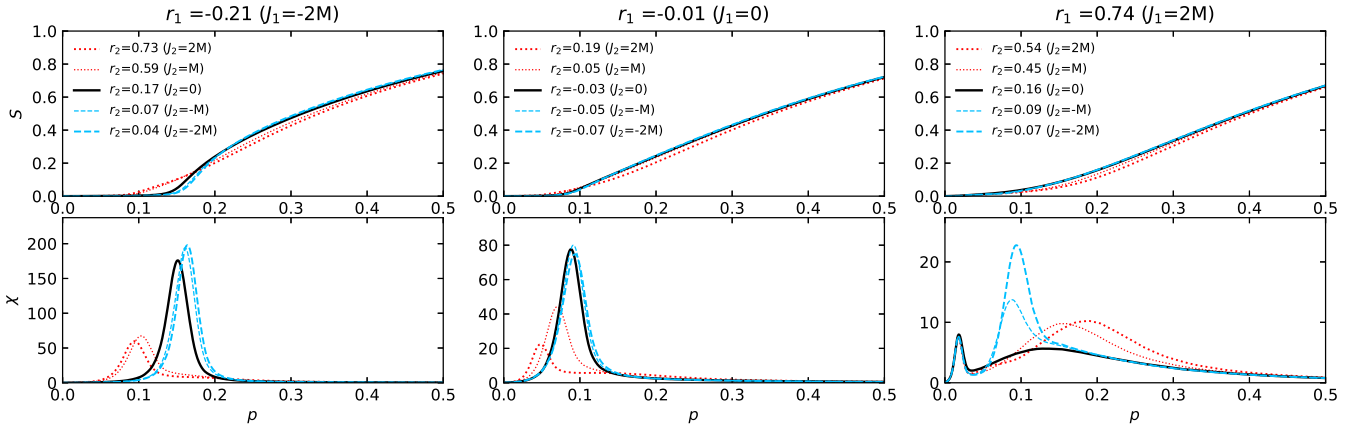


FIG. 3: Here we plot the same information as Fig 2 for the set of 2-NNCRNs from Fig 1(b).

nodes, determining the position of p_c . The second peak can be interpreted as the percolation into the periphery of the giant component and is closely related to the size of R .

Note moreover that for different values of r_2 the relative order of $S(p)$ flips at a certain crossing point, i.e., up to that point the giant connected component with large r_2 is larger than the one corresponding to the network with small r_2 , while the reverse holds above the crossing point. In particular, for large value of p the giant component size grows more slowly and is smaller with larger r_2 . The two regions before and after the crossing point are aggregated into a single number R . Thus, when discussing the relationship between 2NNCRNs and robustness, it is necessary to look at both measurements, $f_{0.005}$ and R .

The two measures $f_{0.005}$ and R used to characterize the robustness of 2-NNCRNs are derived from Figs 2–3 and the result is summarized in Fig 4. We observe that $f_{0.005}$ increases with r_2 (or remains constant in the case of assortative power-law networks), which means that the effect of perturbing r_2 in the positive/negative direction away from r_2^{ext} is to make the network more robust/fragile. Conversely, R tends to decrease with increasing r_2 , which means that r_2 has a negative effect on robustness quantified by R . Quantitatively, the size of the shift in the robustness measures resulting from a change in r_2 is comparable to the effect of a change in r_1 , as explained in the caption of Fig 4. The shift induced by r_2 is especially large in cases where the range of r_2 is wide, such as Poisson networks with $r_1 = 0.00$ or power-law networks with $r_1 = -0.74$.

Unlike most other cases, no change in $f_{0.005}$ due to r_2 is observed in power-law networks with a strongly positive r_1 . This is because strong positive correlations under high degree fluctuations (with $\gamma = 2.5$) induce a core-structure in networks. For any positive p , a component of macroscopic size can be created by connections within the core and

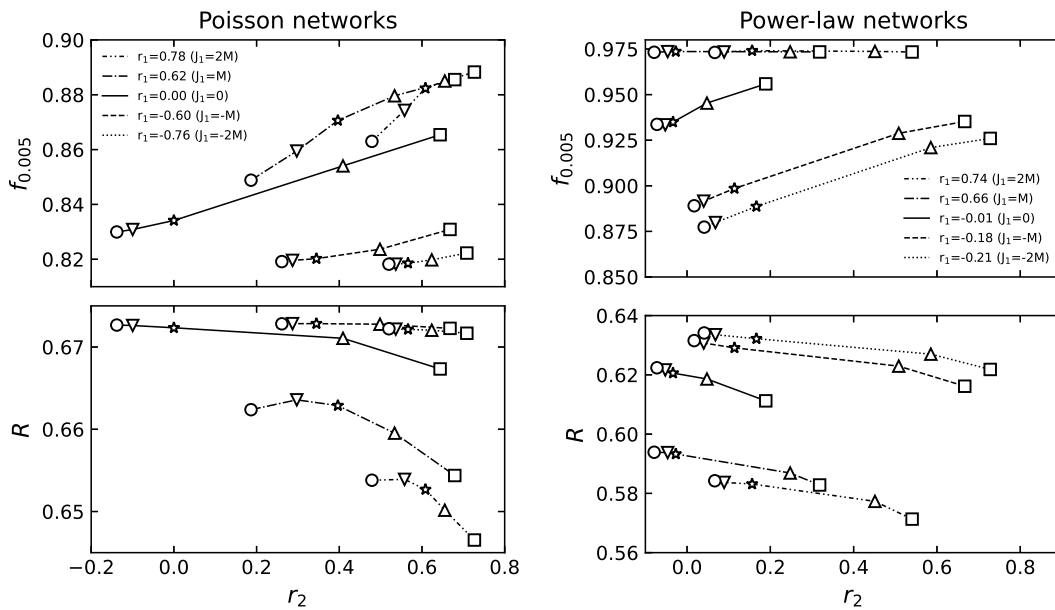


FIG. 4: Robustness of 2-NNCRNs against random edge removal. The symbols indicate the parameter J_2 and are the same as those in Fig 1, whereas lines connect points corresponding to 2-NNCRNs with the same r_1 and the line type corresponds to J_1 . We note that the change in response to varying r_2 (the vertical displacement between the endpoints of a line) is comparable to the response to varying r_1 (the vertical distance between a pair of lines).

to the neighborhood of the core, hence p_c is pushed towards 0 and f_c towards 1 as the network size grows. The invariance of $f_{0.005}$ suggests the change in r_2 due to our algorithm cannot dismantle this core.

We have also performed the same analysis for random node failure, instead of edge failure. The results are similar and are summarized in Fig 5.

C. Targeted attack

It is known that networks that are robust against random failures can still be vulnerable to targeted attacks, where nodes are removed in order of decreasing degree, in particular in random networks with power-law degree distribution [21, 22]. On the other hand, when robustness is evaluated by f_c , it is possible to be robust against both random failure and targeted attacks in networks with positive r_1 [26]. Here, we investigate how the r_2 -dependence of robustness against targeted attacks differs from the case of random failure.

Figs 6–7 depict how the giant component size S and the susceptibility χ depend on the fraction p of surviving nodes under a targeted attack on the same 2-NNCRNs used in Figs 2–3. Fig 8 contains the corresponding values of $f_{0.005}$ and R .

We observe that $f_{0.005}$ increases with r_2 for a fixed choice of r_1 and that this behavior qualitatively matches our observation in the case of random edge failure. Quantitatively, the strength of the shift in $f_{0.005}$ in response to a change in r_2 is stronger than in the case of random failure. Moreover, as in the case of random failure, the size of the shift in response to a change in r_2 is somewhat weaker compared to a change in r_1 .

On the other hand, as observed from the bottom panels in Fig 8, there is a slight increase in R with respect to r_2 , which is more pronounced in power-law networks. We note that the direction of change in R in response is opposite to what we observed in random failure. This difference in behavior is due to the fact that, while there is still a crossing point between $S(p)$ similar to the discussion in Sec. IIIB, it occurs at a higher proportion $S(p)$ of surviving nodes than in the case of random failure. Thus the values of R are influenced more by the behavior of the curves around p_c and we expect that the change in R more closely matches the change in $f_{0.005}$.

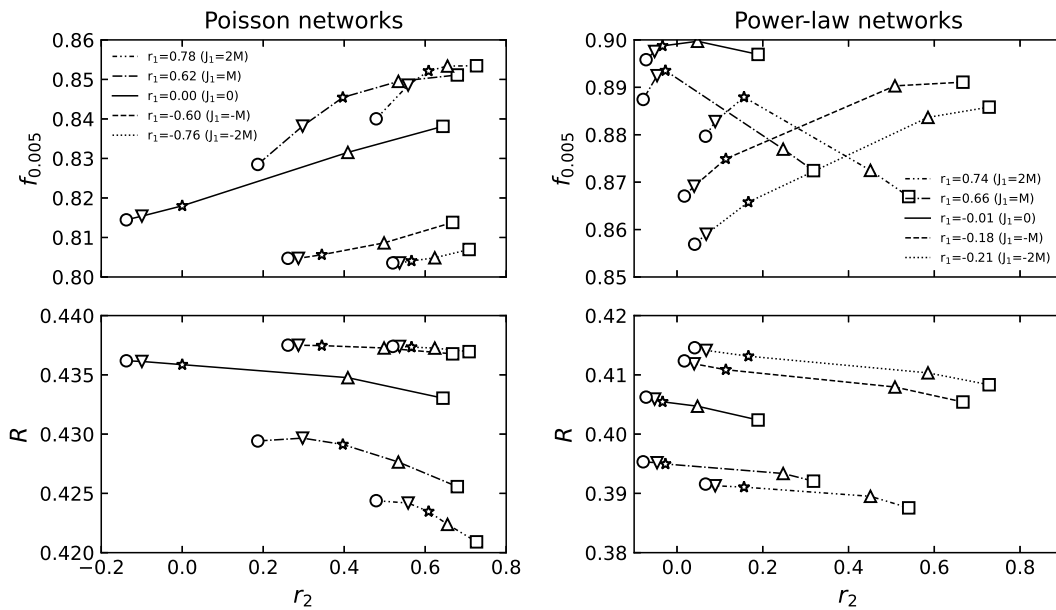


FIG. 5: Robustness of 2-NNCRNs against random node removal, analogously to Fig 4. It is notable that the behavior of $f_{0.005}$ in the top-right panel does not match what has been observed in the case of edge failure or targeted attacks. We believe this is merely an artifact of our choice to approximate p_c by $p_{0.005}$, which is somewhat unstable in cases where the critical point is close to zero.

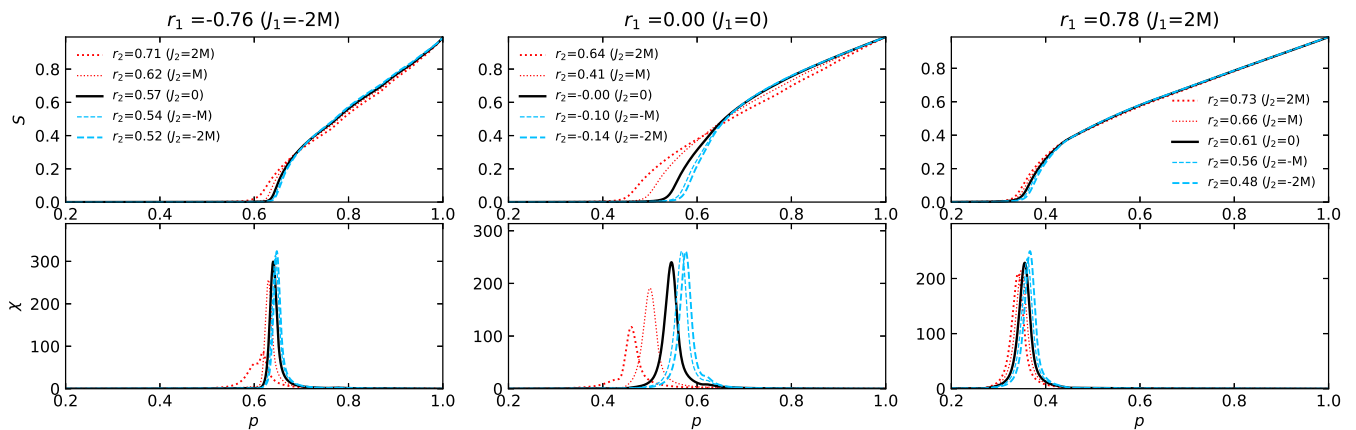


FIG. 6: This plot replicates the information from Fig 2 (Poisson networks) for the case of targeted attack.

IV. CONCLUSION AND DISCUSSION

In this study, we have conducted numerical investigations into the structural properties of networks exhibiting degree-degree correlations between second-nearest neighbors, i.e., long-range degree correlations (LRDCs) at shortest path distance $l = 2$.

To achieve this, we have introduced l -th nearest-neighbor correlated random networks (l -NNCRNs), which exhibit degree-degree correlations up to the l -th nearest neighbor scale while being maximally random at any further scale. We have generated 2-NNCRNs using a two-step algorithm based on random edge rewiring and the Metropolis-Hastings algorithm for two representative degree sequences: Poisson and power-law distributions. Quantifying the strength of the LRDC at distance l using Pearson's correlation coefficient r_l , this two-step algorithm generates 2-NNCRNs with identical r_1 but varying r_2 . Finally, we have investigated the robustness of the networks by simulating random node/edge failures and degree-based targeted attacks.

We have observed that the robustness quantified by $f_{0.005}$ is an increasing function of r_2 when r_1 is held constant

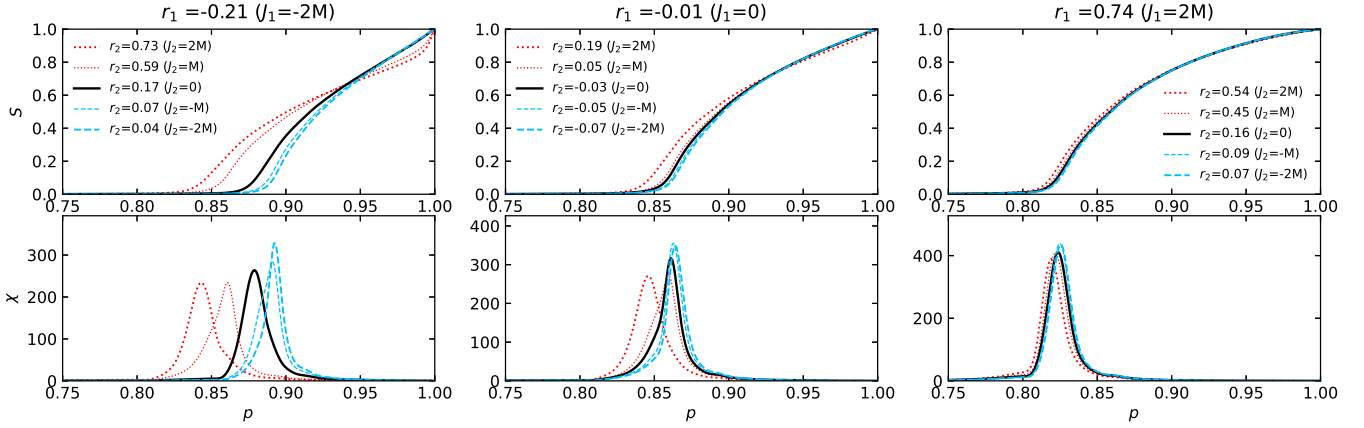


FIG. 7: This plot replicates the information from Fig 3 (power-law networks) for the case of targeted attack.

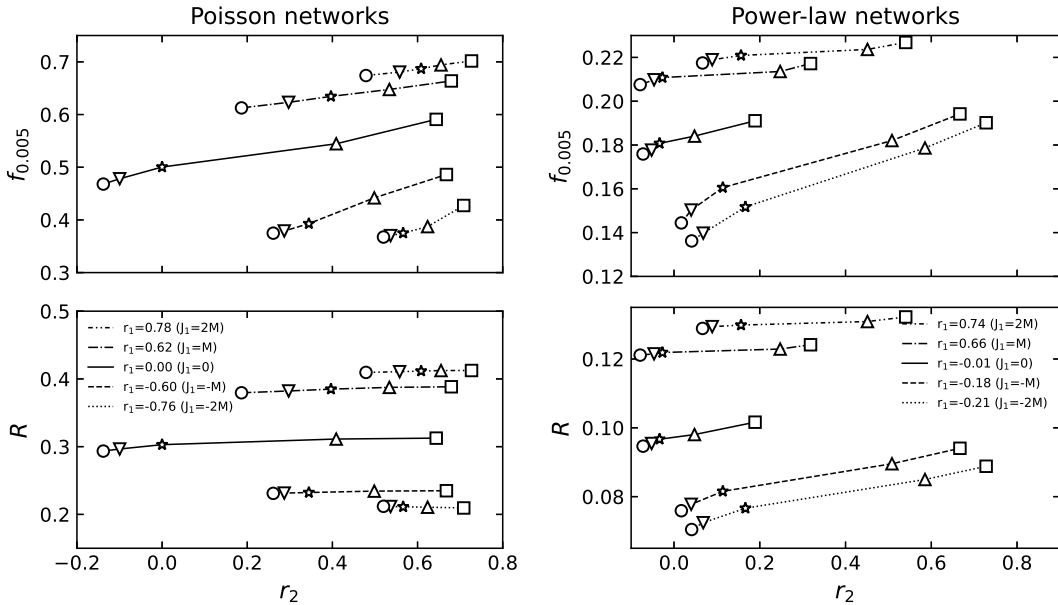


FIG. 8: Robustness of 2-NNCRNs against targeted attack, analogously to Figs 4-5.

in the all cases we simulated (Figs 4, 5 and 8). Thus, networks with smaller (larger) r_2 than r_2^{ext} have been observed to be more fragile (more robust) against both random failure and targeted attack. On the other hand, the effect of r_2 on network robustness, when measured by R , is more nuanced. In the case of bond percolation (Fig 4), R decreases as r_2 exceeds r_2^{ext} , indicating that the network becomes more fragile. However, in the case of targeted attacks (Fig 8), R remains constant or increases slightly with r_2 . This contrasts with our findings when robustness is quantified by $f_{0.005}$ and can be explained by the crosspoint-effect mentioned in Section III B.

To summarize, our numerical results suggest that network robustness is correlated with r_2 when r_1 is fixed, as shown in Table 1. The trends in the influence of r_2 on robustness are similar to those of r_1 . As seen in Figs 4, 5, and 8, the magnitude of the effect caused by changes in r_2 is roughly half of that caused by r_1 , except in the case of R during targeted attacks. This highlights the significant role of second-neighbor degree-degree correlations in network resilience.

In conclusion, if r_1 is kept fixed, then r_2 has a similar effect on robustness as r_1 . To give some explanation of this effect, we have plotted in Fig 9 the size of the k -core in power-law networks with strongly positive r_1 or r_2 and we observe that both constraints lead to quite similar values. To interpret this, recall that the k -core is the part of the network where the giant component starts to emerge as p approaches p_c from below and is thus intimately related to the robustness of the network. Quantitatively, the effect of r_2 on robustness is smaller than r_1 but comparable.

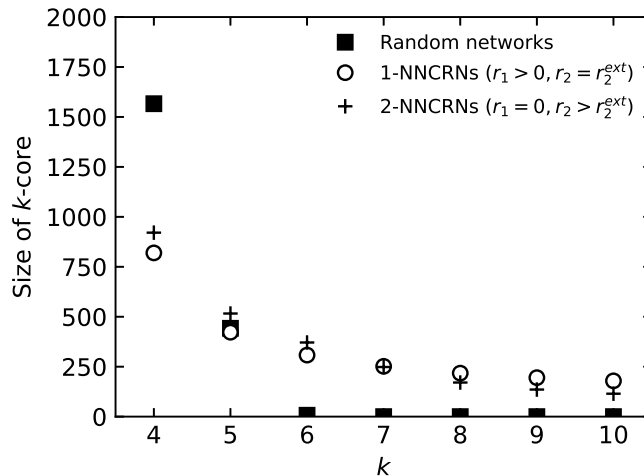


FIG. 9: Size of k -cores in power-law networks with different degree correlations. The values are averaged over 100 configurations. Symbols represent different rewiring parameters: solid squares for $(J_1, J_2) = (0, 0)$, open spheres for $(J_1, J_2) = (2M, 0)$, and crosses for $(J_1, J_2) = (0, 2M)$, which means that the networks are random networks, 1-NNCRNs, and 2-NNCRNs, respectively.

It is natural to expect that LRDCs at $l = 2$ also play an important role in the robustness of a real-world network. Indeed, Fig 10 summarizes the observed values of r_2 for real-world networks and the value of r_2^{ext} for a 1-NNCRN with the same $P(k, k'|l = 1)$. Overall, real-world networks tend to have larger r_2 than r_2^{ext} , and thus our results suggest that intrinsic LRDCs at $l = 2$ in real-world networks contribute positively to structural robustness. It remains an important problem for future work to quantify the influence of LRDCs in such networks.

The insights gained from our study have important implications for the construction of more robust social systems and the development of effective contact rules to mitigate the spread of infectious diseases. Our results show that r_2 significantly affects network robustness, with its positive impact explained by the k -core structure induced when $r_2 > r_2^{\text{ext}}$. Given that nonzero r_1 has emerged as a fundamental property of network structure, influencing not only network robustness but also various dynamic processes and functions, it is likely that r_2 plays a similar role. Further investigations are needed to explore the influence of r_2 on other dynamic processes.

ACKNOWLEDGMENTS

The authors thank S. Mizutaka, T. Hasegawa, and K. Yakubo for fruitful discussions. This work was supported by a Grant-in-Aid for Scientific Research (No. 23K13010 and 23K12984) from the Japan Society for the Promotion of Science.

-
- [1] A.-L. Barabási and R. Albert, *Science* (80-.). **286**, 509 (1999).
 - [2] M. E. J. Newman, *Phys. Rev. Lett.* **89**, 208701 (2002).
 - [3] S. N. Dorogovtsev, A. V. Goltsev, and J. F. F. Mendes, *Rev. Mod. Phys.* **80**, 1275 (2008).
 - [4] R. Pastor-Satorras, C. Castellano, P. Van Mieghem, and A. Vespignani, *Rev. Mod. Phys.* **87**, 925 (2015).
 - [5] Y. Fujiki, T. Takaguchi, and K. Yakubo, *Phys. Rev. E* **97**, 062308 (2018).
 - [6] Y. Fujiki and K. Yakubo, *Phys. Rev. E* **101**, 032308 (2020).

	$p_{0.005}$	$f_{0.005}$	R
Random node/edge failure	↓	↑	↓
Degree-based target attack	↓	↑	↑

TABLE I: Summary of effects of an increase in either r_1 or r_2 on $p_{0.005}$, $f_{0.005}$, and R .

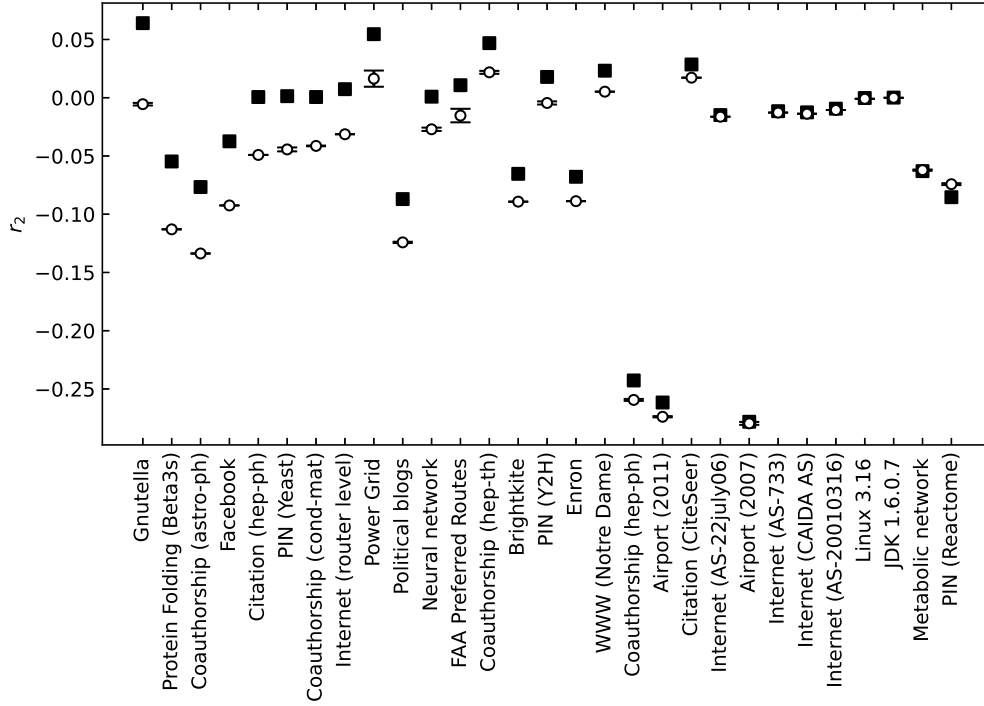


FIG. 10: LRDCs at $l = 2$ in real networks in Table II. Solid squares represent the r_2 -values for real-world networks. Open circles denote r_2^{ext} calculated as the average r_2 values over 100 realizations of the corresponding 1-NNCRNs, with error bars indicating the standard deviation.

- [7] B. Tadić, S. Thurner, and G. J. Rodgers, Phys. Rev. E **69**, 036102 (2004).
- [8] D. Rybski, H. D. Rozenfeld, and J. P. Kropp, EPL (Europhysics Lett. **90**, 28002 (2010).
- [9] M. Boguñá, C. Castellano, and R. Pastor-Satorras, Phys. Rev. Lett. **111**, 068701 (2013).
- [10] R. E. Boulos, A. Arneodo, P. Jensen, and B. Audit, Phys. Rev. Lett. **111**, 118102 (2013).
- [11] L. W. Swanson, O. Sporns, and J. D. Hahn, Proc. Natl. Acad. Sci. **113**, 201613184 (2016).
- [12] Y. Fujiki, S. Mizutaka, and K. Yakubo, Eur. Phys. J. B **90**, 126 (2017).
- [13] S.-C. Ngo, A. G. Percus, K. Burghardt, and K. Lerman, Proc. R. Soc. A Math. Phys. Eng. Sci. **476**, 1 (2020).
- [14] M. E. J. Newman, SIAM Rev. **45**, 167 (2003).
- [15] R. Albert and A.-L. Barabási, Rev. Mod. Phys. **74**, 47 (2002).
- [16] R. Cohen and S. Havlin, Introduction, in *Complex Networks: Structure, Robustness and Function* (Cambridge University Press, 2010) p. 1–6.
- [17] X. Liu, D. Li, M. Ma, B. K. Szymanski, H. E. Stanley, and J. Gao, Phys. Rep. **971**, 1 (2022).
- [18] O. Artime, M. Grassia, M. De Domenico, J. P. Gleeson, H. A. Makse, G. Mangioni, M. Perc, and F. Radicchi, Nat. Rev. Phys. **6**, 114 (2024).
- [19] M. Molloy and B. Reed, Random Struct. Algorithms **6**, 161 (1995).
- [20] D. S. Callaway, M. E. J. Newman, S. H. Strogatz, and D. J. Watts, Phys. Rev. Lett. **85**, 5468 (2000).
- [21] R. Albert, H. Jeong, and A.-L. Barabási, Nature **406**, 378 (2000).
- [22] R. Cohen, K. Erez, D. Ben-Avraham, and S. Havlin, Phys. Rev. Lett. **86**, 3682 (2001).
- [23] A. V. Goltsev, S. N. Dorogovtsev, and J. F. F. Mendes, Phys. Rev. E **78**, 051105 (2008).
- [24] Y. Shiraki and Y. Kabashima, Phys. Rev. E **82**, 036101 (2010).
- [25] H. J. Herrmann, C. M. Schneider, A. A. Moreira, J. S. Andrade Jr, and S. Havlin, J. Stat. Mech. Theory Exp. **2011**, P01027 (2011).
- [26] T. Tanizawa, S. Havlin, and H. E. Stanley, Phys. Rev. E **85**, 046109 (2012).
- [27] C. M. Schneider, A. A. Moreira, J. S. Andrade, S. Havlin, and H. J. Herrmann, Proc. Natl. Acad. Sci. **108**, 3838 (2011).
- [28] M. Mayo, A. Abdelzaher, and P. Ghosh, Comput. Soc. Networks **2**, 4 (2015).
- [29] A. Arcagni, R. Grassi, S. Stefani, and A. Torriero, Eur. J. Oper. Res. **262**, 708 (2017).
- [30] R. Xulvi-Brunet and I. M. Sokolov, Phys. Rev. E **70**, 066102 (2004).
- [31] J. D. Noh, Phys. Rev. E **76**, 026116 (2007).
- [32] C. Orsini, M. M. Dankulov, P. Colomer-de Simón, A. Jamakovic, P. Mahadevan, A. Vahdat, K. E. Bassler, Z. Toroczkai, M. Boguñá, G. Caldarelli, S. Fortunato, and D. Krioukov, Nat. Commun. **6**, 8627 (2015).
- [33] R. Taylor, SIAM J. Algebr. Discret. Methods **3**, 114 (1982).

Network	N	M	Ref.
Airport (2007)	500	2,980	[44, 45]
Airport (2011)	1,574	17,215	[46]
Brightkite	58,228	214,078	[47, 48]
Citation (CiteSeer)	384,054	1,736,145	[49, 50]
Citation (hep-ph)	34,546	420,877	[47, 51, 52]
Coauthorship (astro-ph)	18,771	198,050	[47, 53]
Coauthorship (cond-mat)	23,133	93,439	[47, 53]
Coauthorship (hep-ph)	12,006	118,489	[47, 53]
Coauthorship (hep-th)	9,875	25,973	[47, 53]
Enron	36,692	183,831	[47, 54, 55]
FAA Preferred Routes	1,226	2,408	[49, 56]
Facebook	63,731	817,035	[57]
Gnutella	10,876	39,994	[47, 53, 58]
Internet (AS-20010316)	10,515	21,455	[59]
Internet (AS-22july06)	22,963	48,436	[60]
Internet (AS-733)	6,474	12,572	[47, 51]
Internet (CAIDA AS)	26,475	53,381	[47, 51]
Internet (router level)	192,244	609,066	[61]
JDK 1.6.0.7	6,434	53,658	[49, 62]
Linux 3.16	30,834	213,217	[49, 62]
Metabolic network	453	2,025	[63, 64]
Neural network	297	2,148	[60, 65, 66]
PIN (Reactome)	6,229	146,160	[49, 67]
PIN (Y2H)	3,023	6,149	[49, 68]
PIN (Yeast)	2,284	6,646	[69, 70]
Political blogs	1,224	16,715	[60, 71]
Power Grid	4,941	6,594	[60, 66]
Protein Folding (Beta3s)	132,167	228,967	[59, 72]
WWW (Notre Dame)	325,729	1,090,108	[47, 73]

TABLE II: Properties of the real networks in Fig 10

- [34] I. Stanton and A. Pinar, *ACM J. Exp. Algorithmics* **17**, 3.1 (2012).
- [35] J. Berg and M. Lässig, *Phys. Rev. Lett.* **89**, 228701 (2002).
- [36] J. Park and M. E. J. Newman, *Phys. Rev. E* **70**, 066117 (2004).
- [37] G. Cimini, T. Squartini, F. Saracco, D. Garlaschelli, A. Gabrielli, and G. Caldarelli, *Nat. Rev. Phys.* **1**, 58 (2019).
- [38] M. E. J. Newman, S. H. Strogatz, and D. J. Watts, *Phys. Rev. E* **64**, 026118 (2001).
- [39] M. Boguñá, R. Pastor-Satorras, and A. Vespignani, *Eur. Phys. J. B - Condens. Matter* **38**, 205 (2004).
- [40] P. Holme, B. J. Kim, C. N. Yoon, and S. K. Han, *Phys. Rev. E* **65**, 056109 (2002).
- [41] M. E. J. Newman and R. M. Ziff, *Phys. Rev. E* **64**, 16 (2001).
- [42] S. Mizutaka and T. Tanizawa, *Phys. Rev. E* **94**, 022308 (2016).
- [43] P. Colomer-de Simón and M. Boguñá, *Phys. Rev. X* **4**, 041020 (2014).
- [44] V. Latora, V. Nicosia, and G. Russo, *Complex Networks: Principles, Methods and Applications* (Cambridge University Press, 2017).
- [45] V. Colizza, R. Pastor-Satorras, and A. Vespignani, *Nat. Phys.* **3**, 276 (2007).
- [46] T. Opsahl, Why anchorage is not (that) important: Binary ties and sample selection, <http://wp.me/poFcY-Vw> (2011).
- [47] J. Leskovec and A. Krevl, SNAP Datasets: Stanford large network dataset collection, <http://snap.stanford.edu/data> (2014).
- [48] E. Cho, S. A. Myers, and J. Leskovec, in *Proceedings of the 17th ACM SIGKDD International Conference on Knowledge Discovery and Data Mining*, KDD '11 (Association for Computing Machinery, New York, NY, USA, 2011) p. 1082–1090.
- [49] T. P. Peixoto, The netzschleuder network catalogue and repository, <https://doi.org/10.5281/zenodo.7839981> (2023).
- [50] K. D. Bollacker, S. Lawrence, and C. L. Giles, in *Proceedings of the Second International Conference on Autonomous Agents*, AGENTS '98 (Association for Computing Machinery, New York, NY, USA, 1998) p. 116–123.
- [51] J. Leskovec, J. Kleinberg, and C. Faloutsos, in *Proceedings of the Eleventh ACM SIGKDD International Conference on Knowledge Discovery in Data Mining*, KDD '05 (Association for Computing Machinery, New York, NY, USA, 2005) p. 177–187.
- [52] J. Gehrke, P. Ginsparg, and J. Kleinberg, *ACM SIGKDD Explor. Newsl.* **5**, 149 (2003).
- [53] J. Leskovec, J. Kleinberg, and C. Faloutsos, *ACM Trans. Knowl. Discov. Data* **1**, 2–es (2007).
- [54] J. Leskovec, K. J. Lang, A. Dasgupta, and M. W., *Internet Mathematics* **6**, 10.1080/15427951.2009.10129177 (2009).
- [55] B. Klimt and Y. Yang, in *First Conference on Email and Anti-Spam (CEAS)* (Mountain View, CA, 2004).
- [56] U. S. F. A. Administration, Air traffic control system command center, <http://www.fly.faa.gov/> (2010).

- [57] B. Viswanath, A. Mislove, M. Cha, and K. P. Gummadi, in *Proceedings of the 2nd ACM SIGCOMM Workshop on Social Networks (WOSN'09)* (2009).
- [58] M. Ripeanu, A. Iamnitchi, and I. Foster, *IEEE Internet Computing* **6**, 50–57 (2002).
- [59] <http://cosinproject.eu/data.html>.
- [60] <https://websites.umich.edu/~mejn/netdata/>.
- [61] C. S. R.-L. T. Measurements, <https://www.caida.org/catalog/datasets/router-adjacencies/>.
- [62] J. Kunegis, in *Proc. 22nd Int. Conf. World Wide Web* (ACM, New York, NY, USA, 2013) pp. 1343–1350.
- [63] <https://webs-deim.urv.cat/~alexandre.arenas/data/welcome.htm>.
- [64] J. Duch and A. Arenas, *Phys. Rev. E* **72**, 027104 (2005).
- [65] J. G. White, E. Southgate, J. N. Thumson, and S. Brenner, *Philosophical Transactions of the Royal Society of London. B, Biological Sciences* **314**, 1 (1986).
- [66] D. J. Watts and S. H. Strogatz, *Nature* **393**, 440 (1998).
- [67] G. Joshi-Tope, M. Gillespie, I. Vastrik, P. D'Eustachio, E. Schmidt, B. de Bono, B. Jassal, G. Gopinath, G. Wu, L. Matthews, S. Lewis, E. Birney, and L. Stein, *Nucleic Acids Research* **33**, D428 (2005).
- [68] J.-F. Rual, K. Venkatesan, T. Hao, T. Hirozane-Kishikawa, A. Dricot, N. Li, G. F. Berriz, F. D. Gibbons, M. Dreze, N. Ayivi-Guedehoussou, N. Klitgord, C. Simon, M. Boxem, S. Milstein, J. Rosenberg, D. S. Goldberg, L. V. Zhang, S. L. Wong, G. Franklin, S. Li, J. S. Albala, J. Lim, C. Fraughton, E. Llamas, S. Cevik, C. Bex, P. Lamesch, R. S. Sikorski, J. Vandenhaute, H. Y. Zoghbi, A. Smolyar, S. Bosak, R. Sequerra, L. Doucette-Stamm, M. E. Cusick, D. E. Hill, F. P. Roth, and M. Vidal, *Nature* **437**, 1173 (2005).
- [69] V. Batagelj and A. Mrvar, Pajek datasets, <http://vlado.fmf.uni-lj.si/pub/networks/data/> (2006).
- [70] D. Bu, Y. Zhao, L. Cai, H. Xue, X. Zhu, H. Lu, J. Zhang, S. Sun, L. Ling, N. Zhang, G. Li, and R. Chen, *Nucleic Acids Research* **31**, 2443 (2003).
- [71] L. A. Adamic and N. Glance, in *Proceedings of the 3rd International Workshop on Link Discovery*, LinkKDD '05 (Association for Computing Machinery, New York, NY, USA, 2005) p. 36–43.
- [72] F. Rao and A. Cafisch, *J. Mol. Biol.* **342**, 299 (2004).
- [73] R. Albert, H. Jeong, and A.-L. Barabási, *Nature* **401**, 130 (1999).